MOLECULAR IMAGING AND BIOLOGY

Mol Imaging Biol (2019) 21:78–85
DOI: 10.1007/s11307-018-1208-9

Published Online: 23 May 2018

RESEARCH ARTICLE

Ultrahigh-Field Quantitative MR Microscopy of the Chicken Eye *In Vivo* Throughout the *In Ovo* Period

Felix Streckenbach,[1] Ronja Klose,[1] Sönke Langner,[2] Inga Langner,[3] Marcus Frank,[4] Andreas Wree,[5] Anne-Marie Neumann,[5] Änne Glass,[6] Thomas Stahnke,[1] Rudolf F. Guthoff,[1] Oliver Stachs,[1] Tobias Lindner[7]

[1]*Department of Ophthalmology, Rostock University Medical Center, Doberaner Straße 140, 18057, Rostock, Germany*
[2]*Institute of Diagnostic and Interventional Radiology, Rostock University Medical Center, Ernst-Heydemann-Str. 6, 18055, Rostock, Germany*
[3]*Section of Hand and Functional Microsurgery, Department of Orthopedic and Trauma Surgery, University Medicine Greifswald, Ferdinand-Sauerbruch-Straße, 17475, Greifswald, Germany*
[4]*Medical Biology and Electron Microscopy Centre, Rostock University Medical Center, Strempelstraße 14, 18055, Rostock, Germany*
[5]*Institute of Anatomy, Rostock University Medical Center, Gertrudenstraße 9, 18057, Rostock, Germany*
[6]*Institute for Biostatistics and Informatics in Medicine and Ageing Research, Rostock University Medical Center, Ernst-Heydemann-Str. 8, 18057, Rostock, Germany*
[7]*Core Facility Small Animal Imaging, Rostock University Medical Center, Schillingallee 69a, 18057, Rostock, Germany*

Abstract

Purpose: Ultrahigh-field MRI (UHF-MRI) with an in-plane spatial resolution of less than 100 μm is known as MR microscopy (MRM). MRM provides highly resolved anatomical images and allows quantitative assessment of different tissue types using diffusion-weighted imaging (DWI). The aim of the present study was to evaluate the feasibility of combined *in vivo* anatomical and quantitative assessment of the developing chicken eye *in ovo*.

Procedures: Thirty-eight fertilized chicken eggs were examined at 7.1 T (ClinScan, Bruker Biospin, Germany) acquiring a dataset comprising T2-weighted anatomical images, DWI, and diffusion tensor imaging. To reduce motion artifacts, the eggs were moderately cooled before and during MR imaging. Two eggs were imaged daily for the entire developmental period, and 36 eggs were examined pairwise at only one time point of the embryonic period. Development of the eye was anatomically and quantitatively assessed.

Results: From the D5 embryonic stage (116–124 h), MRM allowed differentiation between lens and vitreous body. The lens core and periphery were first identified at D9. DWI allowed quantification of lens maturation based on a significant decrease in apparent diffusion coefficient values and course of fractional anisotropy. Repeated moderate cooling had no influence on the development of the chicken embryo.

Conclusions: MRM allows *in vivo* assessment of embryonic development of the chicken eye *in ovo* without affecting normal development. The method provides anatomical information supplemented by quantitative evaluation of lens development using DWI. With increasing

Correspondence to: Tobias Lindner; *e-mail:* tobias.lindner@med.uni-rostock.de

availability of ultrahigh-field MR systems, this technique may provide a noninvasive complementary tool in the field of experimental ophthalmology.

Key words: MR microscopy, Eye development, Animal models, Embryology, Ophthalmology, Diffusion MRI, Chick

Introduction

The chicken embryo is an established animal model in the field of ophthalmological research [1]. However, until recently, embryos had to be euthanized for further analysis, thus precluding serial longitudinal evaluation of the same embryo [2]. Magnetic resonance imaging (MRI) provides excellent soft tissue contrast in conjunction with multiplanar imaging capabilities [3] and has recently been used for avian embryo imaging [2]. Ultrahigh-field MRI (UHF-MRI) with a spatial resolution of less than 100 µm is known as MR microscopy (MRM) [4, 5]. MRM yields highly resolved anatomical images comparable to conventional histology in terms of resolution [6]. This makes MRM suitable for studying avian embryology. Especially, the eye with its different soft tissues and its high water content is amenable to evaluation by MRM [4, 5]. However, due to the long imaging time [4], MRM is prone to motion artifacts. Previous studies have demonstrated that external cooling of the embryo may reduce these artifacts while not interfering with normal development [2].

Diffusion-weighted imaging (DWI) allows *in vivo* assessment of water diffusion [3] and is an established technique of ophthalmic imaging [7–9]. Furthermore, diffusion parameters, such as fractional anisotropy (FA) derived from diffusion tensor imaging (DTI) and quantitative apparent diffusion coefficient (ADC) parameter maps calculated from DWI datasets [10, 11], allow characterization of the tissue microstructure. Recent studies indicate that DTI/DWI allows quantification of water diffusion of the lens in animals and humans *in vitro* [7–9] and *in vivo* [12–14].

The purpose of the present proof-of-principle study was to evaluate *in vivo* MRM with DWI and DTI for longitudinal anatomical and quantitative assessment of the embryonic development of the chicken eye *in ovo*.

Materials and Methods

Animal Model

All animals were handled in accordance with the ARVO statement for the Use of Animals in Ophthalmic and Vision Research, and the experiments complied with national legislation for the protection of animals. Thirty-eight fertilized chicken eggs (White Leghorn), obtained from a commercial hatchery (Valo BioMedia, Osterholz-Scharmbeck, Germany), were stored at room temperature (20 °C) for 3 days prior to the starting of incubation. All eggs were simultaneously incubated (Heka-Turbo 168, HEKA, Rietberg, Germany) at optimal conditions: 37.8 °C and 60 % relative humidity as recommended by the manufacturer of the incubator. The eggs were divided into two groups: two eggs were scanned every day (group A), and 36 eggs (group B) were scanned only at one time point between day 1 to day 20 (two eggs at each time point). In the latter group, incubation was terminated at the indicated time points, and the eggs were opened. After euthanization, the length of the third toe was determined to check for normal development according to the staging of Hamburger and Hamilton [15]. None of the embryos hatched.

MR Imaging

In vivo MRM was performed on a 7.1-T MRI scanner (ClinScan, Bruker Biospin, Ettlingen, Germany) with a bore size of 13 cm using a 16-channel volume coil (rat body coil, Bruker Biospin) and a small surface loop coil with 3-cm diameter (s1 coil, Bruker Biospin) for signal detection. During the first 10 days, a fast T2-weighted (T2w) localizer was acquired using the volume coil to identify the chick's position in the egg. If necessary, the position of the egg was modified and the position of the embryo's eyes was marked on the shell for faster localization on follow-up imaging with the surface coil. From day 11, with increasing size of the embryo, the surface coil was used for fast acquisition of T2w localizers, and the coil position was corrected as required. Following the localizer, high-resolution T2w turbo spin-echo sequences of the orbits were acquired in axial and coronal planes. Imaging parameters were time of repetition (TR)/time of echo (TE) 2100/48 ms; matrix size 512×512, interpolated to 1024×1024; field of view (FOV) 38×38 mm; in-plane resolution 0.078×0.078 mm; slice thickness 0.7 mm; no slice gap; time of acquisition (TA), 12:15 min. Next, an axial DWI dataset was acquired using a spin-echo echo-planar imaging sequence (imaging parameters: TR/TE 9500/85 ms; matrix 128×128, interpolated to 256×256; FOV 38×38 mm; in-plane resolution 0.273×0.273 mm; slice thickness 0.7 mm, no slice gap; b-values of 400/800/1000 s/mm^2; TA, 3:20 min), followed by acquisition of a DTI dataset with the same spatial orientation (imaging parameters: TR/TE 14500/88 ms; matrix 154×154, interpolated to 308×308; FOV 38×38 mm; in-plane resolution 0.247×0.247 mm; slice thickness 0.5 mm, no slice gap; b-values of 0/1000 s/mm^2; 20 gradient directions; TA, 4:48 min). Total imaging time was 20:23 min.

From embryonic stage D10 onward, image quality of the fast localizers began to deteriorate due to motion artifacts. Therefore, eggs beyond the D10 stage were bedded on crushed ice 10 min prior to the start and during MRM to reduce artifacts resulting from embryo movement. Cooling was monitored using a fiber-optic thermometer (Model 1025T, Monitoring & Gating System, Small Animal Instruments, USA), and the surface temperature of the egg was reduced to 11.8° prior to imaging.

Image Evaluation

For image analysis, MR datasets were transferred to an Osirix workstation (Vers. 6.0.2). Apparent diffusion coefficient FA parameter maps were calculated using the ADCmap [11] and DTImap [10] plugins. For data analysis, the contours of the lens, the vitreous body, and the entire globe were manually defined on all slides of raw data (see Fig. 1). These contours were then copied as regions-of-interest (ROIs) and transferred to the complete diffusion-weighted dataset including ADC- and FA-map. ADC and FA values were determined for all ROIs and MR datasets. To evaluate reproducibility of the analysis, this procedure was repeated three times, and mean values were calculated for each ROI. For assessment of lens maturation, the contour of the lens on day 5 was considered as lens core. This contour was transferred to all subsequently acquired datasets, allowing differentiation between the central core and the peripheral parts of the lens.

Toe Length Evaluation

In group B, the embryos were euthanized after a single MR imaging examination and the length of the third toe was measured as described by Hamburger and Hamilton [15]. Measurements were taken manually from day 10 to day 20 of incubation to determine the developmental stage [16] using published reference values [15].

Tissue Preparation and HE Staining for Ganglion Cell Counting

Retinal ganglion cell counting was performed for two embryos of each group at the D20 stage as described in Lindner, et al. [16]. For evaluation, all nuclei and total cell numbers of the retinal ganglion layer were estimated using Cavalieri's method.

Statistical Analysis

FA and ADC values are provided as mean ± standard deviation (SD). To evaluate the influence of time on FA and ADC course in an exploratory sense, we introduced an early

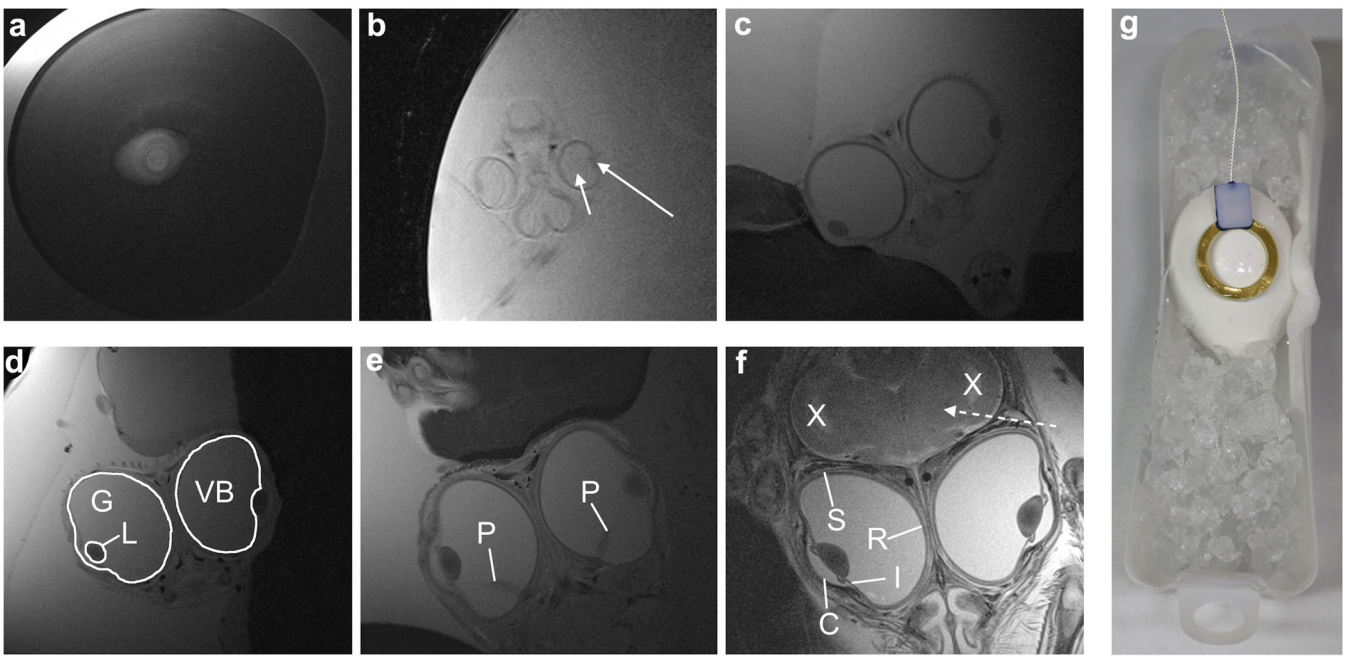

Fig. 1. Anatomical assessment of the developing eye. Axial T2w images of an embryo of group A. **a** At day 1, it was possible to detect inner structures of the egg. **b** At day 5, it was possible to differentiate between lens (arrow) and globe (short arrow). **c** At day 8, the eye diameter is around 5–6 mm. **d** At day 11, examples of globe (G), lens (L), and vitreous body (VB) ROIs are shown. **e** At day 15, the pecten oculi (P), a comb-like structure of blood vessels, is apparent. **f** At day 19, detailed anatomic structures are displayed (x, lateral ventricles; dashed arrow, cortex of the frontal brain; C, cornea; I, iris; S, sclera; R, retina). **g** The egg just before the MRI examination. It is cooled by crushed ice and the surface loop coil is placed.

(D5–D10), middle (D11–D15), and late (D16–D20) phase of development. Differences between the early and late phase, as well as between groups A and B, were assessed using the *U* test by Mann and Whitney, both for left and right side (two-sided, $\alpha = 0.05$, IBM® SPSS® Advanced Statistics 22.0). All results obtained in the rerun of left and right side were quite similar, as expected.

Results

MR Microscopy

All eggs were successfully incubated. MRM identified changes of inner-egg structures from embryonic stage day 1 (D1, 20–28 h) onward. At the D3 stage (68–76 h), the globe was detectable. At the D5 stage (116–124 h), MRM allowed differentiation of the lens and vitreous body (Fig. 1). The pecten oculi were identified from D6 (140–148 h) onward (Fig. 1).

Quantitative Image Analysis

Quantification of DWI was possible from embryonic stage D5 onward. Since our data revealed no differences in ADC (lens and vitreous body as well) between groups A and B for each of the development phases "early," "middle," and "late" ($p > 0.05$ each), we merged the ADC values of both groups for description of ADC course in lens and vitreous body for further evaluation. ADC value of the entire lens was $(1.38 \pm 0.01) \times 10^{-3}$ mm^2/s and decreased to $(0.60 \pm 0.10) \times 10^{-3}$ mm^2/s at the D19 stage (Fig. 2, $p < 0.05$ between early and late phase of development). Differentiation between the lens core and lens periphery on diffusion-weighted images was possible at embryonic stage D9 (212–220 h). At this stage, mean ADC of the lens core was $(0.94 \pm 0.09) \times 10^{-3}$ mm^2/s and of the lens periphery $(1.33 \pm 0.07) \times 10^{-3}$ mm^2/s. The ADC decreased to $(0.09 \pm 0.04) \times 10^{-3}$ mm^2/s for the core and to $(0.64 \pm 0.06) \times 10^{-3}$ mm^2/s for the periphery until D19 (see Fig. 3). From D19 onward, ADC values remained stable until the calculated day of hatching.

ADC of the vitreous body was $(1.87 \pm 0.03) \times 10^{-3}$ mm^2/s at embryonic stage D5 and decreased to $(1.48 \pm 0.02) \times 10^{-3}$ mm^2/s by D19 to then remain constant (Fig. 4). This decrease could be shown to be significant ($p < 0.05$, "early" *vs.* "late").

FA values of the vitreous body were 0.07 ± 0.01 at the D5 stage and then stabilized around 0.09 ± 0.02 until D19 (Fig. 4). In contrast, FA values of the lens showed initially 0.18 ± 0.01 (stage D5), with a clear increase during lens development to 0.46 ± 0.04 at D19 (Fig. 2, $p < 0.05$ "early" *vs.* "late").

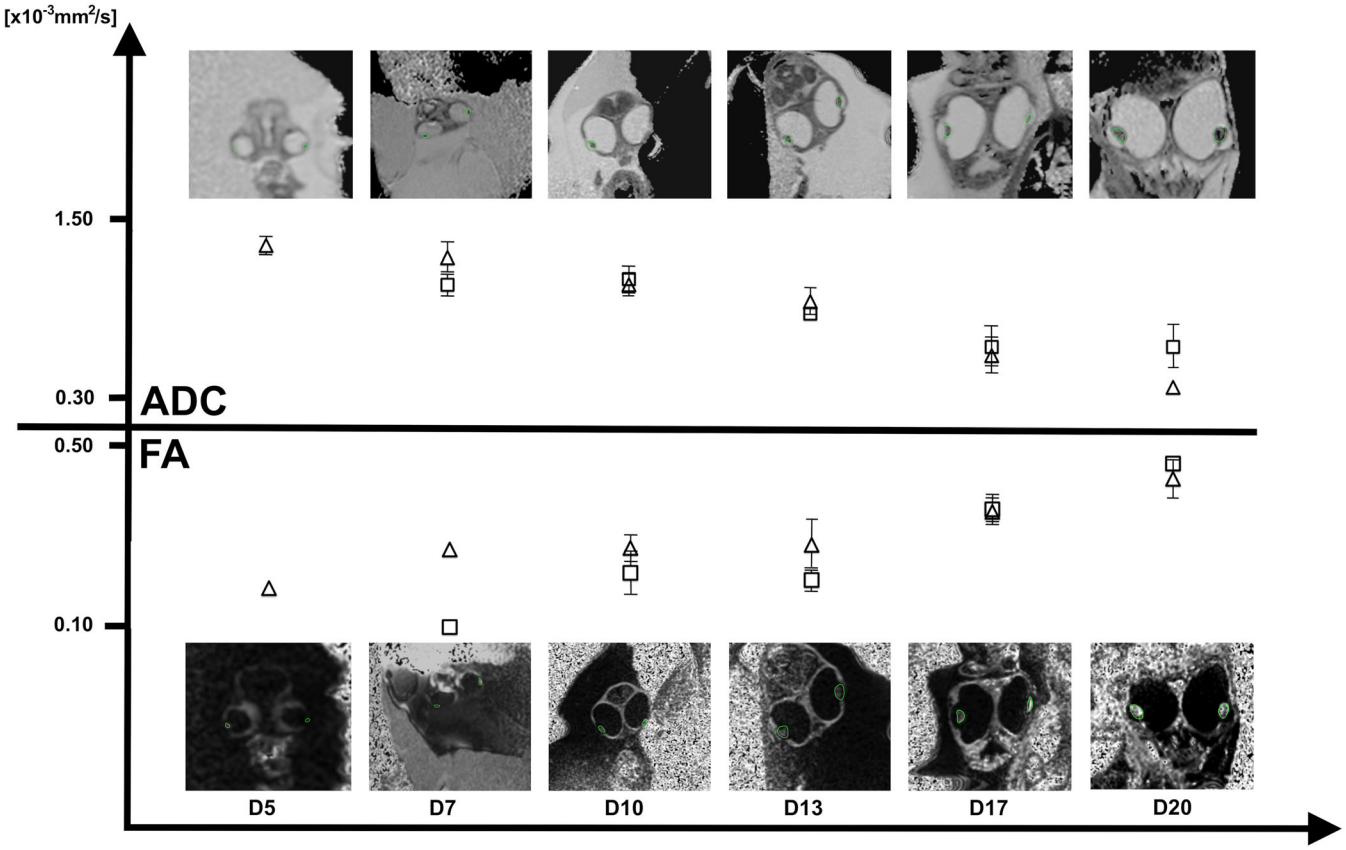

Fig. 2. ADC and FA of the developing lens (group A, □; group B, △). Maturation of the lens leads to a decrease in ADC values and an increase in FA values as the ultrastructural complexity of the lens increases ($p < 0.05$ early *vs.* late phase).

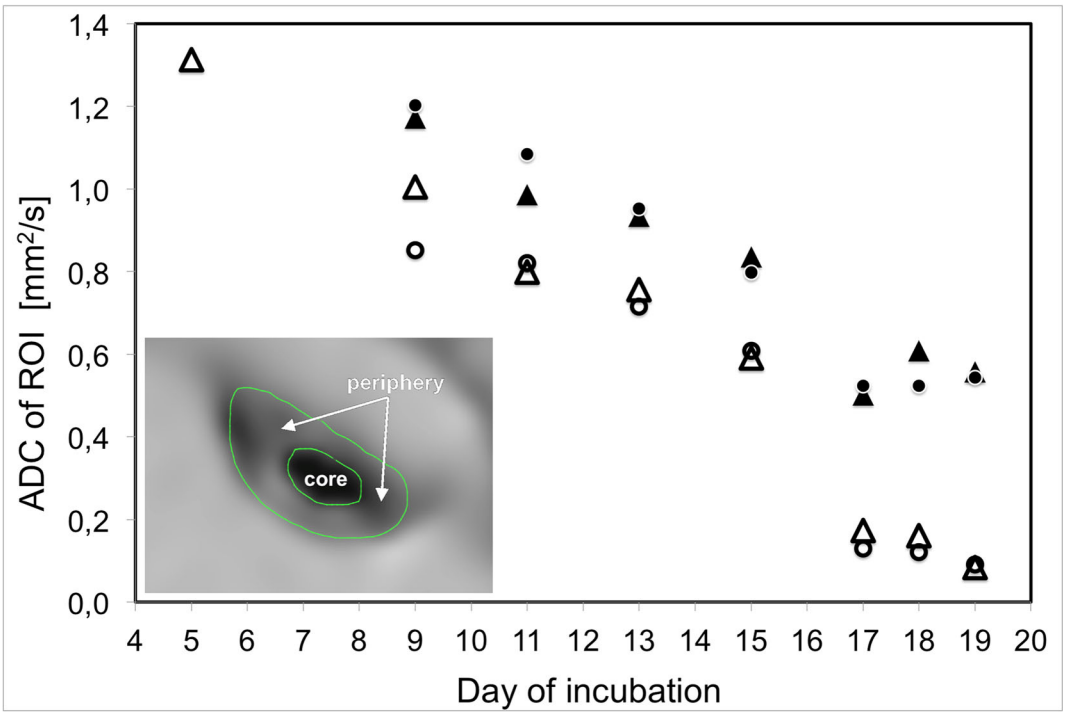

Fig. 3. ADC of the lens center (group A, ○; group B, △) and lens periphery (group A, ●; group B, ▲) by day of incubation. The developing ultrastructure in the central and peripheral parts of the lens leads to decreasing ADC values, with a stronger decrease in the core.

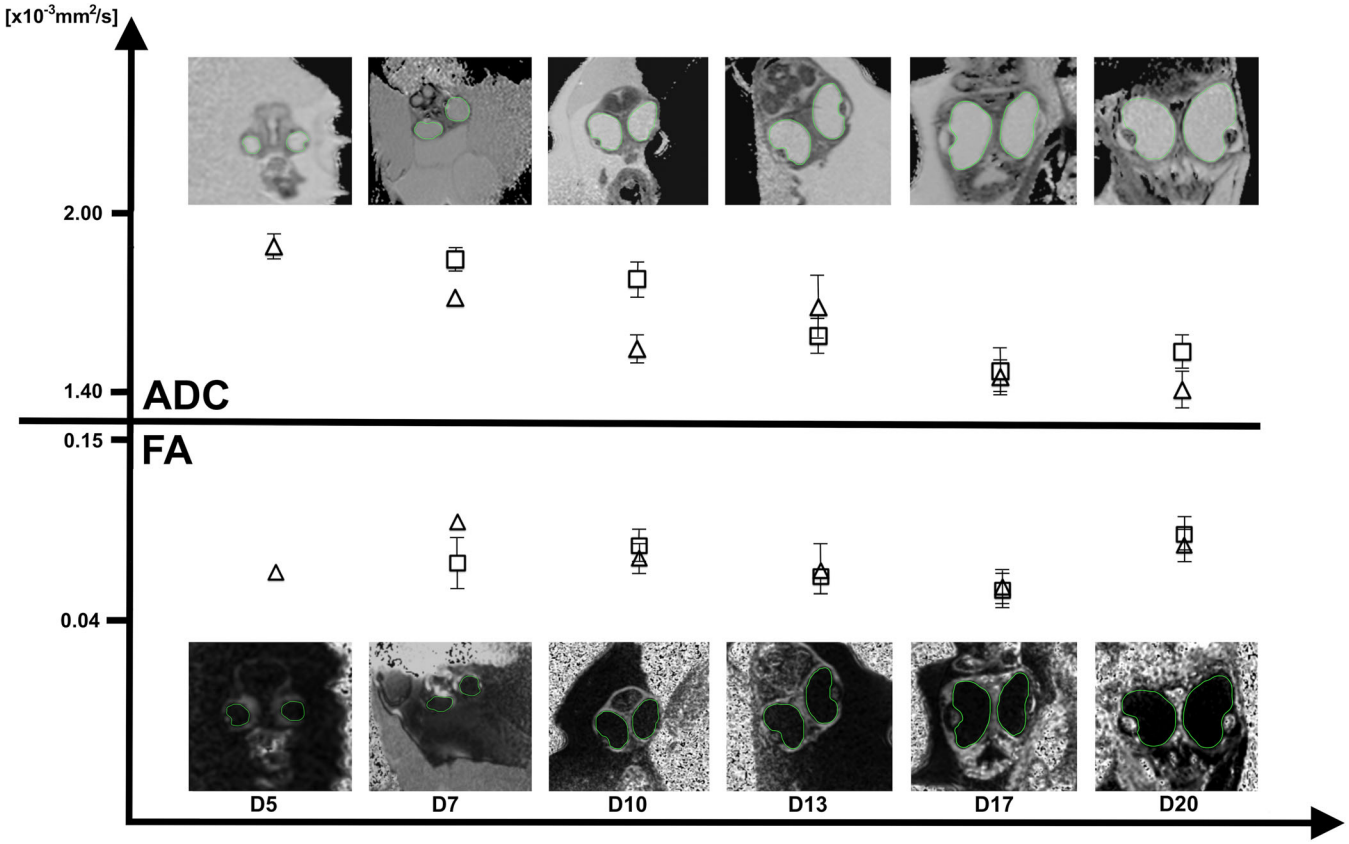

Fig. 4. ADC and FA of the developing vitreous body (group A, □; group B, △). Increasing protein content of the vitreous body results in lower ADC values ($p < 0.05$ early *vs.* late phase). However, this is not associated with an increase in ultrastructural complexity and thus there is no increase in FA.

The length of the third toe was 6.0 mm on day 10 (Hamburger and Hamilton (HH) stage 36) and 22.5 mm on day 20 (HH stage 45). These lengths were in the range of previously reported values [15], as was the length of the third toe at the other stages of embryonic development (Fig. 5a). Length of the third toe also did not differ between the two groups at the last comparable embryonic stage (D20) as same as the ADC value during the entire development process (Fig. 5b). Total cell counts (mean of two eyes) were estimated in the chick embryo retinal ganglion layer at D20 under both experimental conditions: 3.79×10^6 in group A and 3.85×10^6 in group B (length of the third toe and cell count data already published in Lindner et al. [16]).

Discussion

Ultrahigh-field MR microscopy is an established imaging technique in experimental ophthalmology [3], providing good correlation with conventional histology [17]. The results of our study show that *in vivo* DWI and DTI of the developing chicken eye *in ovo* is feasible. We achieved an in-plane spatial resolution of DWI and DTI of 273×273 µm and 247×247 µm, respectively, which is superior to previous *in vitro* [8] and *in vivo* [14] animal studies.

In vivo studies of the human lens by Bilgili et al. show a tendency toward increasing ADC values with age [14]. The authors postulate that this may be attributable to a loss of proteins such as collagen and proteoglycans with aging. This is in accordance with the results of our study. We found a decrease in ADC values from embryonic stages D5 through D19, consistent with the formation of proteins and consequently less molecular movement during lens maturation [18]. This is in agreement with the changes in FA values during lens development. FA is a scalar parameter derived from diffusion-weighted datasets and describing the anisotropy of diffusion in the tissue evaluated [19]. From early to late embryonic stages, there was an increase in FA of the lens indicative of a developing ultrastructure of the lens. From the D9 stage onward, the central core and the peripheral parts of the lens could be differentiated by DWI and DTI, consistent with embryonic eye lens development. During lens development, the lens core is becoming compacted due to the apposition of lens fibers in the periphery. In the equatorially located germinative zone, mitotically active epithelial cells evolve into fiber cells, which add to the existing layers [18, 20, 21]. Compaction of the lens is associated with a decrease in free water motion and hence a decrease in ADC values. The increasing ultrastructural complexity of the lens leads to a decrease in the isotropy of water motion within the lens and is reflected in increasing FA values.

ADC values in the vitreous body decreased from embryonic stages D5 through D15 and then stabilized until D20. This decrease in free water movement is caused by a continuous gain of proteins in the developing vitreous body [22]. However, there was no increased in ultrastructural complexity, which is why FA values of the vitreous body were nearly constant throughout the developmental period.

T2w and diffusion tensor images are relatively long and are therefore prone to motion artifacts. These artifacts can be

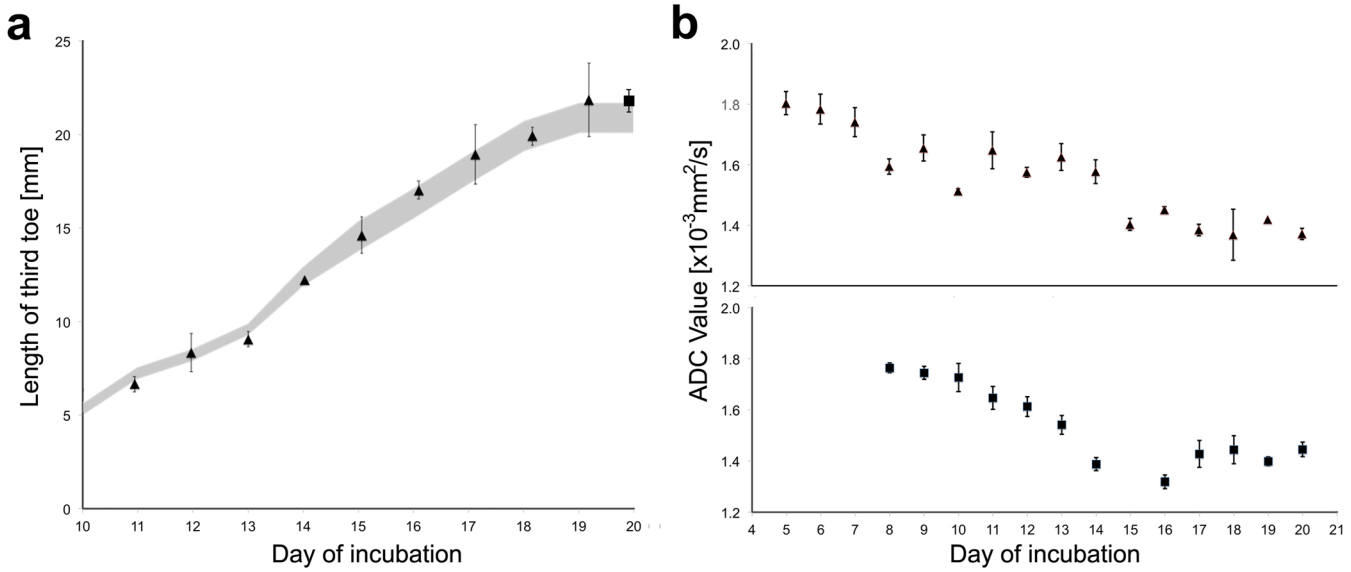

Fig. 5. Impact of cooling and MR imaging on the development of chicken embryos. **a** Relationship between length of third toe (gray, normal stages Hamburger V and Hamilton HL (1951); length of third toe of population B in this study, ▲; population A, ■) and incubation day. The lengths measured in the embryos of group B ($n = 2$) are mostly within the reference range. The lengths measured in group A, despite daily scanning and repeated cooling of the eggs, are also within the reference range and close to those measured in group B. **b** Relationship between ADC of total eye (group A, ■; group B, ▲) and incubation day. No significant difference in molecular movement inside the eye between group A and group B could be detected ($p > 0.05$, left and right likewise).

reduced by cooling of the egg [23]. Possible adverse effects of repeated cooling on chicken development, as discussed by previous studies [24], have not been confirmed by the results of our study. The length of the third toe of the embryos of group A was within the published range [15] of normal embryonic development. Additionally, cell counts in the retinal ganglion layer also rule out an impact of cooling or MRI on chick development in our study.

Our study has some limitations. While the spatial resolution of MRM is still inferior to that of conventional histology [25], its major advantage over histological workup is its noninvasiveness. Furthermore, with the functional information of DWI and DTI, MRM provides further insights into the ultrastructure of the tissue comparable to *in situ* hybridization techniques or immune stains. Although DTI is used in clinical routine for fiber tracking, spatial resolution did not allow visualization of the course of the optic nerve in our experimental setting. However, this limitation can be overcome with improvement of coil technology, increased field strength, and optimization of the sequences used for DTI [13, 26]. Finally, the number of embryos used in this proof-of-principle study is small. A further limitation is the cooling of the eggs. At the one hand, cooling is necessary to prevent motion artifacts; on the other hand, cooling is influencing water diffusion. As it is known that the diffusion of water molecules is temperature dependent [27], cooling of the eggs reduces the calculated ADC values. To correct for this decreased ADC values of lens and vitreous body, it would be necessary to know the actual temperature of lens and vitreous body or knowing the ADC of lens and vitreous body at another temperature (*e.g.*, 37.8 °C) for the same time point. In our study, we only measured the egg shell temperature (11.8 °C) and therefore do not know the temperatures of lens and vitreous body. However, for future studies, it is necessary to cool the eggs at any time point and additional measure the ADC of a structure which does not change over the *in ovo* development.

Conclusion

In conclusion, our explorative study shows that combined anatomical and quantitative *in vivo* assessment of the developing avian eye *in ovo* is possible using MRM. With increasing availability of ultrahigh-field MR systems, this technique may provide an accurate, noninvasive complementary tool in the field of experimental ophthalmology and the evaluation of embryonic development.

Acknowledgements. The authors gratefully thank Mr. Stefan Hadlich for performing the MRI examinations and providing general technical support during the experiment.

Authors' Contributions. Conception and design: SL, OS, and TL. Acquisition of data: FS, RK, AMN, TS, SL, and TL. Analysis and interpretation of the data: IL, TS, AW, AG, OS, SL, and TL. Statistical analysis: AG. Drafting of the article: FS, TL, and SL. Critical revision of the article for important intellectual content: FS, RK, SL, IL, TS, MF, AW, AMN, RFG, OS, and TL. Final approval of the article: FS, RK, SL, IL, TS, MF, AW, AMN, RFG, OS, and TL. Provision of study materials: OS and SL. Responsibility for the integrity of the work as a whole: OS, SL, and TL.

Compliance with Ethical Standards

Ethics Approval

All animals were handled in accordance with the ARVO statement for the Use of Animals in Ophthalmic and Vision Research, and the experiments complied with national legislation for the protection of animals.

Availability of Data and Materials

The raw imaging data is stored at the author's PACS system and will be available in DICOM format upon request.

Conflict of Interest

The authors declare that they have no conflict of interest.

References

1. Schaeffel F, Feldkaemper M (2015) Animal models in myopia research. Clin Exp Optom 98:507–517
2. Bain MM, Fagan AJ, Mullin JM, McNaught I, McLean J, Condon B (2007) Noninvasive monitoring of chick development in ovo using a 7T MRI system from day 12 of incubation through to hatching. J Magn Reson Imaging 26:198–201
3. Niendorf T, Paul K, Graessl A et al (2014) Ophthalmological imaging with ultrahigh field magnetic resonance tomography: technical innovations and frontier applications. Klin Monatsbl Augenheilkd 231:1187–1195
4. Lindner T, Langner S, Graessl A, Rieger J, Schwerter M, Muhle M, Lysiak D, Kraus O, Wuerfel J, Guthoff RF, Falke K, Hadlich S, Krueger PC, Hosten N, Niendorf T, Stachs O (2014) High spatial resolution in vivo magnetic resonance imaging of the human eye, orbit, nervus opticus and optic nerve sheath at 7.0 Tesla. Exp Eye Res 125:89–94
5. Langner S, Krueger P-C, Lindner T, Niendorf T, Stachs O (2014) In vivo MR microscopy of the human eye. Klin Monatsbl Augenheilkd 231:1016–1022
6. Hosten N, Zimpfer A, Guthoff R et al (2013) Experimental differentiation of intraocular masses using ultrahigh-field magnetic resonance imaging—a case series. PLoS One 8:8–13. https://doi.org/10.1371/journal.pone.0081284
7. Vaghefi E, Donaldson PJ (2013) An exploration into diffusion tensor imaging in the bovine ocular lens. Front Physiol 1:1–11
8. Changb C (2000) High-resolution MR imaging rabbit of water lens diffusion. Exp Eye Res 54:127–132
9. Moffat BA, Pope JM (2002) Anisotropic water transport in the human eye lens studied by diffusion tensor NMR micro-imaging. Exp Eye Res 74:677–687
10. Hargreaves B, Sung K, Moseley M (2015) DTI map. http://deqiang.webege.com/software/OsirixPlugins/DTIMap.html
11. Sung K, Charles-Edwards G (2015) ADC map calculation V1.9. https://web.stanford.edu/~bah/software/ADCmap/
12. Cheng H-M (2002) Water diffusion in the rabbit lens in vivo. Dev Ophthalmol 35:169–175
13. Ho LC, Sigal IA, Jan N-J et al (2016) Non-invasive MRI assessments of tissue microstructures and macromolecules in the eye upon biomechanical or biochemical modulation. Sci Rep 6. https://doi.org/10.1038/srep32080
14. Bilgili Y, Meral I (2011) Diffusion changes in the vitreous humor of the eye during aging. Am J Neuroradiol 32:1563–1566
15. Hamburger V, Hamilton H (1951) A series of normal stages in the development of the chick embryo. J Morphol 88:49–92
16. Lindner T, Klose R, Streckenbach F et al (2017) Morphologic and biometric evaluation of chick embryo eyes in ovo using 7 Tesla MRI. Sci Rep 7. https://doi.org/10.1038/s41598-017-02755-4
17. Krueger P-C, Stachs O, Hadlich S, Falke K, Erbersdobler A, Hosten N, Langner S (2012) MR microscopy of the human eye at 7.1 T and correlation with histopathology-proof of principle. Orbit 31:390–393
18. Augusteyn RC (2007) Growth of the human eye lens. Mol Vis 13:252–257

19. Le Bihan D, Mangin J-F, Poupon C et al (2001) Diffusion tensor imaging: concepts and applications. J Magn Reson Imaging 13:534–546
20. Augusteyn RC (2014) Growth of the eye lens: I. Weight accumulation in multiple species. Mol Vis 20:410–426
21. Augusteyn RC (2008) Growth of the lens: in vitro observations. Clin Exp Optom 91:226–239
22. Beebe DC, Latker CH, Jebens HAH, Johnson MC, Feagans DE, Feinberg RN (1986) Transport and steady-state concentration of plasma proteins in the vitreous humor of the chicken embryo: implications for the mechanism of eye growth during early development. Dev Biol 114:361–368
23. Xu J, Delproposto Z, Zhou Z et al (2012) In ovo monitoring of smooth muscle fiber development in the chick embryo: diffusion tensor imaging with histologic correlation. PLoS One 7:1–8. https://doi.org/10.1371/journal.pone.0034009
24. Wilson MESHR, Mcpherson BN, Mather FB et al (1996) Low temperature effects on embryonic development and hatch time. Poult Sci 75:924–932
25. Langner I, Stahnke T, Stachs O, Lindner T, Kühn JP, Kim S, Wree A, Langner S (2016) MR microscopy of the human fetal upper extremity—a proof-of-principle study. BMC Dev Biol 16:21. https://doi.org/10.1186/s12861-016-0123-z
26. Göbel K, Gruschke OG, Leupold J, Kern JS, Has C, Bruckner-Tuderman L, Hennig J, von Elverfeldt D, Baxan N, Korvink JG (2015) Phased-array of microcoils allows MR microscopy of ex vivo human skin samples at 9.4 T. Skin Res Technol 21:61–68. https://doi.org/10.1111/srt.12157
27. Hasegawa Y, Latour LL, Sotak CH, Dardzinski BJ, Fisher M (1994) Temperature dependent change of apparent diffusion coefficient of water in normal and ischemic brain of rats. J Cereb Blood Flow Metab 14:383–390